*Comput. Math. Applic.* Vol. 16, No. 4, pp. 297–305, 1988
Printed in Great Britain. 

0097-4943/88 $3.00 + 0.00


# BUOYANCY-INDUCED FLOWS IN POROUS MEDIA

C.-A. WANG
Department of Applied Mathematics, National Chiao Tung University, Hsinchu, Taiwan 30050, R.O.C.

(*Received* 14 *January* 1988)

Communicated by E. Y. Rodin

**Abstract**—A steady-state model concerning the buoyancy-induced plane flows in porous media saturated with cold pure water is studied. By applying the finite-difference method, two families of solutions are found which exhibit the behavior of unidirectional flows near the impermeable vertical isothermal surface. A gap, with varying ambient temperature, is found where none of the solutions corresponding to upward or downward flows exists. Without applying the boundary-layer approximation, the results show that the steady-state model gives no indication of the flows when the ambient temperature lies inside the gap.

## NOMENCLATURE

$c_p$ = Specific heat
$g$ = Gravitational acceleration
$g_1, g_2, g_3$ = Coefficients in some expressions
$k$ = Thermal conductivity
$K$ = Permeability of porous media
$n$ = Porosity of porous materials
$q$ = Exponent in density relation
$R$ = Temperature ratio
$s$ = Salinity
$t$ = Temperature
$u$ = Darcy velocity in the $x$-direction
$v$ = Darcy velocity in the $y$-direction
$\mathbf{V}$ = Velocity vector
$x$ = Coordinate tangential to the impermeable surface
$y$ = Coordinate normal to the impermeable surface
$\alpha_1$ = Thermal-diffusivity ratio
$\mu$ = Viscosity of the fluid
$\rho$ = Density
$\psi$ = Stream function

*Subscripts*

e = Effective quantities of porous media
f = Quantities of fluid
m = Quantities at the extremes
r = Quantities at the reference condition
s = Quantities of porous material
0 = Quantities at the interface
$\infty$ = Quantities at infinity

## 1. INTRODUCTION

In the natural world, we frequently encounter transport process in fluids where the motion is driven by the interface of a difference in density in a gravitational field. The occurrence of a motion-driven buoyancy effect may arise from a density difference caused by a temperature difference. Also, as in oceanic circulation, the difference in salinity may further affect the density differences. Therefore, the buoyancy force is the stimulus to the fluid flow, particularly in oceanic circulation. All such occurrences are similar and termed "natural convection".

The buoyancy effect arises from the action of a body force, usually gravity, on density differences in a body of fluid. The density differences are the result of temperature or species-concentration differences which are controlled by the nature of the diffusion processes. Thus, all diffusions may be simultaneously occurring and interacting with each other. The consequence is that all aspects of the flow and diffusive processes must be considered simultaneously. The mechanisms of such

flows are further complicated by the occurrence of density extrema as the temperature varies. It is known that a density extremum is reached at about 4°C in pure water at atmospheric pressure. Density extrema also occur in saline water up to a salinity level of about 26 ppt (parts per thousand) and at elevated pressures up to 300 bar-abs.

Such mechanisms also occur in saturated media such as permeable soils flooded by cold lake or sea water, or water slurries, since density extrema may occur in this situation as well. There are a number of experimental or theoretical studies [1–14] in connection with porous media. In these studies, the fluid density is assumed to be varied linearly with temperature. However, this is inapplicable for water at low temperatures. Thus, Gebhart and Mollendorf [15] developed a new density relation for pure or saline water by imposing the temperature extrema. Moreover, Ramilison and Gebhart [16], by applying the new density relation, presented a study on the problem of transport of porous media saturated with pure or saline water at low temperatures.

A temperature ratio $R$ is introduced [16], $R = (t_\infty - t_m)/(t_0 - t_m)$, where $t_\infty$, $t_0$ and $t_m$ denote the temperature, respectively, at ambient, at the vertical surface and at the occurrence of density extrema. With $R$, Ramilison and Gebhart [16], Gebart *et al.* [17], and Hastings and Kazarinoff [18], have reported numerically or mathematically that there is a gap, $0.19 < R < 0.4$, for which no steady-state similarity solution is found. A similar gap has been found in both numerical and mathematical studies of a vertical ice surface melting in a porous medium saturated with cold pure and saline water [19]. Moreover, various theoretical and numerical studies on buoyancy-induced flows in pure or saline water show the existence of a similar gap.

Combining these studies, for either Newtonian or non-Newtonian steady-state flows, it is found that both the flow and buoyancy force are upward if $R < 0$ and downward if $R > 1/2$. For $R$ ranging from 0 to 1/2, two distinct flow regimes with local buoyancy force reversal across the thermal-diffusion region have also been found. The first regime is upward flow, as in Fig. 1(a), and the second regime, as in Fig. 1(b), is downward flow. Flows with $R$ close to zero correspond to the first regime and those with $R$ close to 1/2 correspond to the latter.

However, the use of boundary-layer approximations, which were applied to obtain similar results in Refs [16–18], in describing the possible behavior of bidirectional flow with the temperature ratio inside the gap is questionable. Therefore, the steady-state model, presented by Ramilison and Gebhart [16], is worth studying to understand the nature of buoyancy-induced flows in porous media saturated with cold pure water.

## 2. ANALYSIS OF THE MODEL

Consider the model of vertical buoyancy-force-driven plane flows imbedded in an extensive porous medium saturated with either pure or saline water under conditions in which density extrema might occur. We take a Cartesian coordinate system with the origin at the leading edge of the flow, as shown in Fig. 1(a, b), where $x$ increases in the downstream direction.

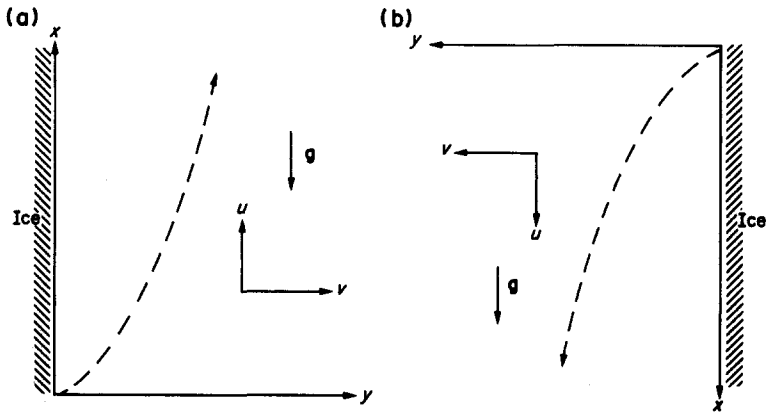


Fig. 1. Coordinate systems for the two flow regimes: (a) mostly upward flow; and (b) mostly downward flow.

To simplify the study, the following hypotheses have been made:

(H1) The physical properties of the fluid and the medium are isotropic and homogeneous.
(H2) Darcy's law, which states that the specific flux vector is proportional to the hydraulic gradient in porous media, is assumed.
(H3) The saturating liquid and porous layer are in local thermodynamic equilibrium.
(H4) The Boussinesq approximation resulting from $\Delta\rho/\rho \ll 1$, where $\rho$ is the density of the saturating liquid in the porous media and $\Delta\rho$ denotes the average change of $\rho$ with respect to temperature, is used.
(H5) There is no salinity diffusion, and the Dufour and Soret effect are both negligible, for small wall-to-ambient temperature differences.

With the above assumptions, the governing equations are given by

$$\nabla\cdot\mathbf{V} = 0, \tag{1}$$

$$\mathbf{V} = \frac{K}{\mu}(\rho\mathbf{g} - \nabla p), \tag{2}$$

$$(\rho_r\cdot c_p)_f\cdot\mathbf{V}\cdot\nabla t = k_e\nabla^2 t, \tag{3}$$

and

$$\rho = \rho_m(s,p)[1 - \alpha(s,p)|t - t_m(s,p)|^q], \tag{4}$$

where $\mathbf{V}$ is the vector of Darcy velocity, $\mu$ and $c_p$ are the viscosity and specific heat of the convective fluid and $\rho_r$ is its density at a reference temperature. Also, $K$ and $k_e$ are, respectively, the permeability and the effective thermal conductivity of the saturated porous medium, $p$ and $\mathbf{g}$ are the fluid pressure and the gravitational acceleration and $s$ is the salinity level of the water.

Moreover, the buoyancy force in equation (2) is calculated from a new density equation (4), where $\rho_m$ and $t_m$ denote the maximum density and temperature for the given pressure and salinity level. The forms and values of $q$, $\alpha$, $\rho_m$ and $t_m$, for the case "$n = 2$" in Ref. [15], are given by

$$\rho(t,s,p) = \rho_m(s,p)\{1 - \alpha(s,p)|t - t_m(s,p)|^{q(s,p)}\},$$

$$\rho_m(s,p) = \rho_m(0,1)\{1 + f_1(p) + sg_1(p)\},$$

$$\alpha(s,p) = \alpha(0,1)\{1 + f_2(p) + sg_2(p)\},$$

$$t_m(s,p) = t_m(0,1)\{1 + f_3(p) + sg_3(p)\},$$

$$q(s,p) = q(0,1)\{1 + f_4(p)\},$$

$$f_i(p) = \sum_{j=1}^{2} f_{ij}(p-1)^j$$

and

$$g_i(p) = \sum_{j=0}^{2} g_{ij}(p-1)^j,$$

where $q(0,1) = 1.894816$, $\rho_m(0,1) = 0.999972\ \mathrm{g\,cm^{-3}}$, $\alpha(0,1) = 9.297173 \times 10^{-6}(^\circ\mathrm{C})^{-q(0,1)}$ and $t_m(0,1) = 4.025^\circ\mathrm{C}$. The constants $f_{ij}$s and $g_{ij}$s are given in Ref. [15]. To simplify the study, we take $p = 1$ bar-abs and $s = 0$ ppt. This yields $q(s,1) = q(0,1)$ and reduces the density correlation to the following:

$$\rho = \rho(t) = \rho(t,0,1) = \rho_m(0,1)\{1 - \alpha(0,1)|t - t_m(0,1)|^{q(0,1)}\}. \tag{5}$$

For a vertical plane flow in a saturated porous medium, $u$ and $v$ are the downstream and normal components of the filtration velocity $\mathbf{V}$. Darcy's law and the equation of energy can be written as

$$u = \frac{K}{\mu}\left(\pm\rho g - \frac{\partial p}{\partial x}\right), \tag{6a}$$

$$v = \frac{-K}{\mu}\frac{\partial p}{\partial y} \tag{6b}$$

and

$$u\frac{\partial t}{\partial x} + v\frac{\partial t}{\partial y} = \frac{k_e}{(\rho_r \cdot c_p)_f}\left(\frac{\partial^2 t}{\partial x^2} + \frac{\partial^2 t}{\partial y^2}\right), \tag{7}$$

where the plus sign in equation (6a) is for the coordinate system shown in Fig. 1(b) and the minus sign is for that in Fig. 1(a). The pressure term in equations (6a, b) can be eliminated through cross-differentiation and then the Darcy's equation can be written as

$$\frac{\partial u}{\partial y} - \frac{\partial y}{\partial x} = \pm\frac{K \cdot g}{\mu}\frac{\partial \rho}{\partial y}. \tag{8}$$

For an impermeable surface at $y = 0$ with a prescribed temperature $t_0$, the appropriate boundary conditions are

$$\text{at the isothermal surface, } y = 0: \quad t = t_0, v = 0$$

$$\text{at the ambient, } y \to \infty: \quad u \to 0, t \to t_\infty. \tag{9}$$

Furthermore, the continuity equation (2) gives the existence of the stream function $\psi(x, y)$ with $\partial\psi/\partial y = u$ and $\partial\psi/\partial x = -v$. Therefore, equations (7) and (9) can be written as follows:

$$\frac{\partial^2 \psi}{\partial x^2} + \frac{\partial^2 \psi}{\partial y^2} = \pm\frac{K}{\mu} \cdot g \cdot \frac{\partial p}{\partial y} \tag{$10^{\pm}$}$$

and

$$\frac{\partial \psi}{\partial y}\cdot\frac{\partial t}{\partial x} - \frac{\partial \psi}{\partial x}\cdot\frac{\partial t}{\partial y} = \alpha_1\left(\frac{\partial^2 t}{\partial x^2} + \frac{\partial^2 t}{\partial y^2}\right), \tag{11}$$

where $\alpha_1 = k_e/(\rho_r \cdot c_p)_f$. The corresponding boundary conditions now become

$$\text{at } y = 0: \quad t = t_0, \frac{\partial \psi}{\partial x} = 0 \tag{12a}$$

$$\text{when } y \to \infty: \quad t \to t_\infty, \frac{\partial \psi}{\partial y} \to 0. \tag{12b}$$

Let $P$ denote the problem with equations (1), (5), (7) and (8), along with conditions (9); and Q denote the problem with equations (5), (10) and (11), along with the associated conditions (12a, b). By observing problems P and Q, problem Q is much more suitable to be studied numerically due to the large amount of grid points which need to be chosen when applying the finite-difference method (FDM). We now turn to discuss the discretization process in the following section. To be more specific, problem $Q^+$ denotes the upward flow problem with equations (5), ($10^+$), (11) and conditions (12a, b), while problem $Q^-$ denotes the downward flow problem governed by equations (5), ($10^-$), (11) and conditions (12a, b).

## 3. DISCRETIZATION

Due to the bounded nature of the FDM, the defined domain for problem Q will be confined on a bounded rectangle $B = \{(x, y) | 0 \leqslant x \leqslant x_\infty, 0 \leqslant y \leqslant y_\infty\}$. The ambient condition (12b) will be imposed on the vertical line $Y_\infty = \{(x, y_\infty) | 0 \leqslant x \leqslant x_\infty\}$. Meanwhile, it is found [16, 17] that the plane flows are driven mainly by the physical conditions at the ambient $y$-direction. Therefore, $x_\infty$ is set at unity in our study.

The discretization process will be given carefully as follows:

Let $\{x_0, \ldots, x_n\}$ and $\{y_0, \ldots, y_m\}$ be the nodes along the $x$- and $y$-directions respectively, with $x_0 = y_0 = 0$, $x_n = x_\infty$, $y_m = y_\infty$. Set $h_i = x_i - x_{i-1}$ and $k_j = y_j - y_{j-1}$. Also $\psi_{i,j}$ and $t_{i,j}$ denote $\psi(x_i, y_j)$ and $t(x_i, y_j)$, respectively.

Assume the uniform meshes $(x_i, y_j)$ are chosen, where $x_i = ih$, $y_j = jk$ with $h = x_\infty/n$ and $k = y_\infty/m$.

Based on the model, the rectangle $B$ is considered to consist of the interior $B'$, the vertical surface line $Y_0 = \{(x, 0) | 0 \leqslant x \leqslant x_\infty\}$, the vertical ambient boundary $Y_\infty = \{(x, y_\infty) | 0 \leqslant x \leqslant x_\infty\}$, the lower horizontal line $X_0 = \{(0, y) | 0 \leqslant y \leqslant y_\infty\}$, the upper horizontal line $X_\infty = \{(x_\infty, y) | 0 \leqslant y \leqslant y_\infty\}$ and two corner points $A = (0, y_\infty)$ and $B = (x_\infty, y_\infty)$. Therefore, the discretization process should be given carefully on these parts. With the local truncation error $O(h^2 + k^2)$, we have following difference equations:

(i) In $B'$: for $1 \leqslant i \leqslant n-1$, $1 \leqslant j \leqslant m-1$,

$$\frac{\psi_{i+1,j} - 2\psi_{i,j} + \psi_{i-1,j}}{h^2} + \frac{\psi_{i,j+1} - 2\psi_{i,j} + \psi_{i-1,j-1}}{k^2} = \pm c \cdot |t_{i,j} - t_m|^{q-1} \frac{t_{i,j+1} - t_{i,j-1}}{2k} \tag{13}$$

and

$$(\psi_{i,j+1} - \psi_{i,j-1})(t_{i+1,j} - t_{i-1,j}) - (\psi_{i+1,j} - \psi_{i-1,j})(t_{i,j+1} - t_{i,j-1}) = 4hk\alpha_1 \left( \frac{t_{i+1,j} - 2t_{i,j} + t_{i,j-1}}{h^2} + \frac{t_{i,j+1} - 2t_{i,j} + t_{i,j-1}}{k^2} \right) \tag{14}$$

where $c = (K/\mu)g\rho_m \alpha q \operatorname{sgn}(t_{i,j} - t_m)$ with $\rho_m = \rho_m(0, 1)$, $\alpha = \alpha(0, 1)$ and $q = 1.894816$.

(ii) On $Y_0$: by conditions (12a), $\partial\psi/\partial x = 0$ and $t = t_0$ on the entire surface, then we have, for $0 \leqslant i \leqslant n$,

$$\frac{\psi_{i,0} - 2\psi_{i,1} + \psi_{i,2}}{k^2} = \pm c\, |t_0 - t_m|^{q-1} \frac{3t_0 - 4t_{i,1} + t_{i,2}}{2h} \tag{15}$$

and

$$t_0 - 2t_{i,1} + t_{i,2} = 0. \tag{16}$$

(iii) On $Y_\infty$: by condition (12b), $\partial\psi/\partial y \to 0$ and $t \to t_\infty$, we have, for $1 \leqslant i \leqslant m-1$,

$$\frac{\psi_{i,m} - 2\psi_{i,m-1} + \psi_{i,m-2}}{k^2} = \pm c \cdot |t_\infty - t_m|^{q-1} \cdot \frac{t_\infty - 4t_{i,m-1} + t_{i,m-2}}{2k} \tag{17}$$

and

$$-(\psi_{i+1,m} - \psi_{i-1,m})(3t_{i,m} - 4t_{i,m-1} + t_{i,m-2}) = 4hk\alpha_1 \left( \frac{t_\infty - 2t_{i,m-1} + t_{i,m-2}}{k^2} \right). \tag{18}$$

(iv) On $X_0$: for $1 \leqslant j \leqslant m-1$,

$$\frac{\psi_{0,j} - 2\psi_{1,j} + \psi_{2,j}}{h^2} + \frac{\psi_{0,j+1} - 2\psi_0 + \psi_{0,j-1}}{h^2} = \pm c \cdot |t_{0,j} - t_m|^{q-1} \frac{t_{0,j+1} - t_{0,j-1}}{2k} \tag{19}$$

and

$$(\psi_{0,j+1} - \psi_{0,j-1})(3t_{0,j} - 4t_{1,j} + t_{2,j}) - (3\psi_{0,j} - 4\psi_{1,j} + \psi_{2,j})(t_{0,j+1} - t_{0,j-1}) = 4hk\alpha_1 \left( \frac{t_{0,j} - 2t_{1,j} + t_{2,j}}{h^2} + \frac{t_{0,j+1} - 2t_{0,j} + t_{0,j-1}}{k^2} \right). \tag{20}$$

(v) On $X_\infty$: for $1 \leqslant j \leqslant m-1$,

$$\frac{\psi_{n,j} - 2\psi_{n-1,j} + \psi_{n-2,j}}{h^2} + \frac{\psi_{n,j+1} - 2\psi_{n,j} + \psi_{n,j-1}}{k^2} = \pm c\, |t_{n,j} - t_m|^{q-1} \frac{t_{n,j+1} - t_{n,j-1}}{2k} \tag{21}$$

and

$$(\psi_{n,j+1} - \psi_{n,j-1})(3t_{n,j} - 4t_{n-1,j} + t_{n-2,j}) - (3\psi_{n,j} - 4\psi_{n-1,j} + \psi_{n-2,j})(t_{n,j+1} - t_{n,j-1}) = 4hk\alpha_1 \left( \frac{t_{n,j} - 2t_{n-1,j} + t_{n-2,j}}{h^2} + \frac{t_{n,j+1} - 2t_{n,j} + t_{n,j-1}}{k^2} \right). \tag{22}$$

(vi) At the point $A = (0, y_\infty)$,

$$\frac{\psi_{0,m} - 2\psi_{1,m} + \psi_{2,m}}{h^2} = \pm c\,|t_\infty - t_m|^{q-1}\left(\frac{3t_\infty - 4t_{0,m-1} + t_{0,m-2}}{2k}\right) \tag{23}$$

and

$$-(3\psi_{0,m} - 4\psi_{1,m} + \psi_{2,m})(3t_\infty - 4t_{0,m-1} + t_{0,m-2}) = 4hk\alpha_1\left(\frac{t_{0,m} - 2t_{0,m-1} + t_{0,m-2}}{k^2}\right). \tag{24}$$

(vii) At the point $B = (x_\infty, y_\infty)$,

$$\frac{\psi_{n,m} - 2\psi_{n-1,m} + \psi_{n-2,m}}{h^2} = \pm c\,|t_\infty - t_m|^{q-1}\left(\frac{3t_\infty - 4t_{n,m-1} + t_{n,m-2}}{2k}\right) \tag{25}$$

and

$$-(3\psi_{n,m} - 4\psi_{n-1,m} + \psi_{n-2,m})(3t_\infty - 4t_{n,m-1} + t_{n,m-2}) = 4hk\alpha_1\left(\frac{t_{n,m} - 2t_{n,m-1} + t_{n,m-2}}{k^2}\right). \tag{26}$$

## 4. NUMERICAL RESULTS AND DISCUSSION

Equations (13)–(26) in Section 3 form a nonlinear system $F(x) = 0$ with $x = (\psi_{0,0}, \ldots, \psi_{n,m}, t_{1,1}, \ldots, t_{1,m-1}, t_{2,1}, \ldots, t_{n-1,m-1})^t$. The quasi-Newton method is applied for solving the given system $F(x) = 0$. Moreover, the matrix inversion formula of Sherman and Morrison is applied to bypass most of the linear system solvers required in the quasi-Newton method except for the first iteration. Such a formula drastically reduces the number of computations and, of course, the run time.

The physical coefficients $c_p$, $\mu$ and $K$ are evaluated, in some explicit forms in Ref. [20], at the reference temperature $t_f = (t_0 + t_\infty)/2$. The effective thermal conductivity $k_e$ is evaluated with the following form [21], by assuming that the porous medium is of series conduction:

$$1/k_e = n/k_f + (1 - n)/k_s,$$

where $n$ denotes the porosity of the saturating solid and $k_f$ and $k_s$ are the thermal conductivity of the saturating fluid and solid, respectively. In this study, due to the lack of experimental data, we assume that the porous medium consists of well-distributed sand stones, with $n = 40\%$ and $k_s = 0.9806 \times 10^{-2}$ cal/cm s °C [22]. Meanwhile, $k_f$ is calculated in an explicit form in Ref. [23] at $t_f$. Also, we assume that the entire vertical surface is uniform with temperature $t_0 = 0$°C.

With the above preparation the numerical computations for the problem of upward flows, problem $Q^+$, were performed on the CYBER 170/720 at NCTU initially with $t_\infty = t_m = 4.025$°C. The initial guesses we take from the similarity results obtained in Ref. [17] with the inverse similarity transformation. By setting the tolerance $\epsilon = 10^{-6}$ in the quasi-Newton method and $h = 0.1$, $k = 1$, $y_\infty = 20$, a solution was obtained with about 25 s CPU time. Then $y_\infty$ was increased to 40, 60 and 80 with the initial data provided by the previous run. The agreement of the solution data was to reach at least three digits when compared at $y = 0$ and $y = y_\infty$. The homotopy continuation technique was then applied to further increase $t_\infty$ from $t_m$ with a step size of 0.05°C. It was found that solutions were obtained for each $t_\infty$ up to 4.975°C, i.e. $R \simeq 0.19$, and the quasi-Newton method failed to converge if $t_\infty \geqslant 5$°C. For the downward flow problem $Q^-$, similar techniques were applied for $t_\infty$ reduced from $2t_m$ with the same step size. By imposing the initial data for $t_\infty = 2t_m$, taken from Ref. [17], it was also found that the lowest level of $t_\infty$ at which a solution was found is 6.7°C, $R \simeq 0.4$. It was also found that a second solution is obtained for each $t_\infty$ ranging from 6.8 to 7.5°C. Moreover, similar to Refs [16] or [17], a gap in $t_\infty$, with $5°C \leqslant t_\infty \leqslant 6.7°C$, was found where neither problem had a solution. However, none of the multiple solutions for the upward flow problem reported in Ref. [17] were found in our study. This was expected since the multiple solutions in Ref. [17] are very similar and our discretization for the model is very approximate in some senses.

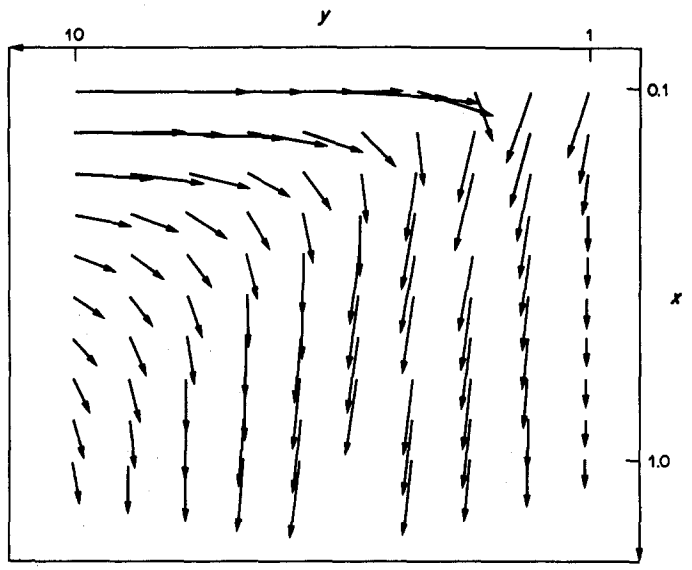


Fig. 2. The Darcy velocity profile for the downward flow problem, with $t_\infty = 8°C$.

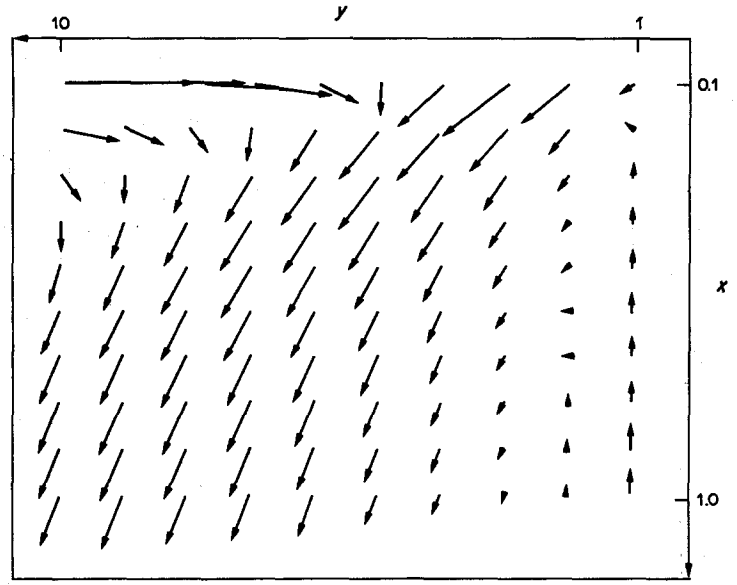


Fig. 3. The Darcy velocity profile for the downward flow problem, with $t_\infty = 7°C$ (first solution).

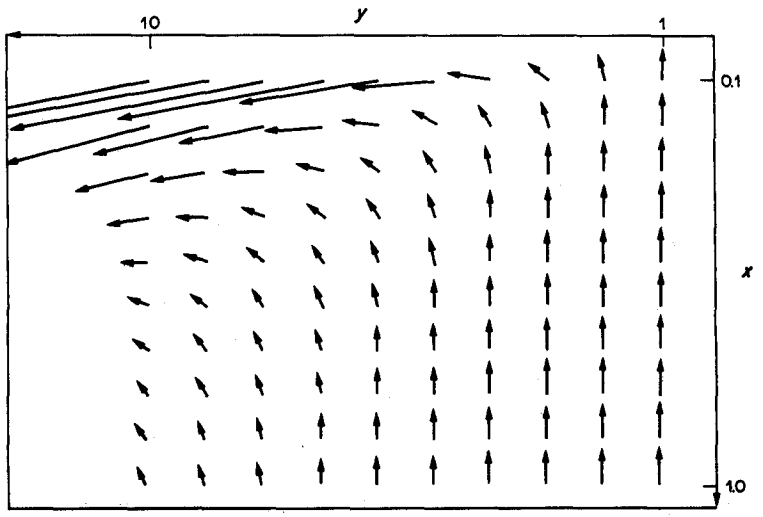


Fig. 4. The Darcy velocity profile for the downward flow problem, with $t_\infty = 7°C$ (second solution).

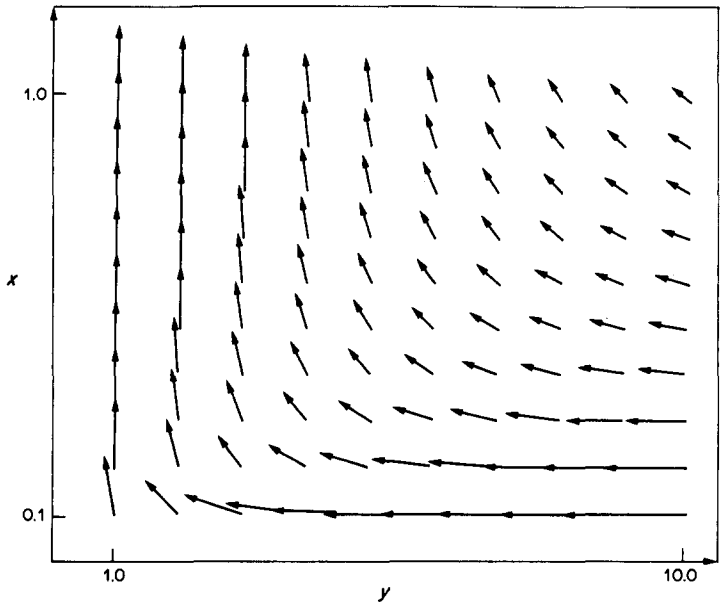


Fig. 5. The Darcy velocity profile for the upward flow problem, with $t_\infty = t_m = 4.025°C$.

Applying the relations $\partial\psi/\partial y = u$ and $\partial\psi/\partial x = v$, various Darcy's velocity $\mathbf{V} = (u, v)$ profiles with $0 < x \leqslant 1$ and $0 < y \leqslant 10$ for selected $t_\infty$s were plotted and are shown in Figs 2–6. The solutions obtained are consistent with those in Ref. [16]. With $R$ close to 1/2 (Fig. 2), flows are mostly downward with positions near the surface, $y = 0$. At $t_\infty = 70°C$, $R \simeq 0.42$, the first solution shows that, the buoyancy forces dominate the upward flows near the surface and result in the occurrence of downward flows with positions away from the surface. Therefore (as in Fig. 3), a boundary layer is found. However (as in Fig. 4), the second solution shows the drastic increase in the thickness of such layer. Similar results are also reported in Ref. [17]. Usually, such a drastic change means instability. For the problem with $t_\infty$ near $t_m$, the buoyancy forces are mainly generated near the surface and then it can be observed that the convection phenomena occur at a position away from the surface, as in Figs 5 and 6. The flows with $t_\infty = t_m$ and $t_\infty = 4.975°C$ are similar.

As mentioned earlier, no steady-state solution is obtained where the ambient temperature $t_\infty$ varies inside the gap, $5°C < t_\infty < 6.7°C$. This is similar to the result reported in Ref. [16]. However,

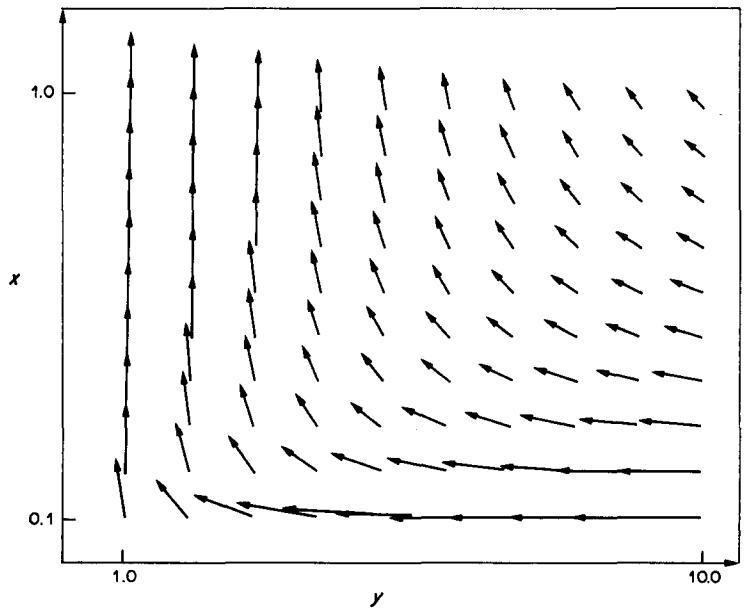


Fig. 6. The Darcy velocity profile for the upward flow problem, with $t_\infty = 4.975°C$.

Ramilison and Gebhart indicated that the boundary-layer approximations applied in Ref. [16] are of questionable use in studying bidirectional flows, especially when the temperature $t_\infty$ varies inside the gap. Our study shows that the complete steady-state model gives no indication of the behavior of any steady-state flows inside the gap region. Unfortunately, we know of no data from experimental measurements concerning transport in porous media. To study the steady flows or the actual occurrence of instability in the downward flow, an extensive experimental study is required which may lead to a new formulation. Moreover, it is worthwhile, in studying the time-dependent version of the present model, to solve the mystery of the buoyancy-induced plane flows inside the gap.

*Acknowledgement*—This work was supported by Grant No. NSC75-0201-N009d-02 of the R.O.C.

## REFERENCES

1. M. Combarnous and B. Lefur, Transfer de chaleur par convection naturelle dans une couche poreuse horizontal. *C.r. hebd. Seanc. Acad. Sci. Paris* **269,** 1009–1012 (1969).
2. J. W. Elder, Steady free convection in a porous medium heated from below. *J. Fluid Mech.* **27,** 29–46 (1967).
3. T. Kaneko, M. F. Mohtadi and K. Aziz, An experimental study of natural convection in inclined porous media. *Int. J. Heat Transfer* **17,** 485–496 (1974).
4. J. P. Caltagirone, M. Cloupeau and M. Combarnous, Convection naturelle fluctuante dans une couche poreuse horizontal. *C.r. hebd. Seanc. Acad. Sci. Paris, Serie B* **273,** 833 (1971).
5. Y. Yen, Effects of density inversion on free convection heat transfer in porous layer heated from below. *J. Fluid Mech.* **17,** 1349–1356 (1974).
6. J. P. Caltagirone, Stabilite d'une couche poreuse horizontale soumise á des conditions aux limites periodiques. *Int. J. Heat Transfer* **19,** 815–829 (1967).
7. D. A. Nield, Onset of convection in a fluid layer overlying a layer of a porous medium. *J. Fluid Mech.* **81,** 573–622 (1977).
8. R. N. Horne and M. J. O'Sullivan, Convection in a porous medium heated from below: the effect of temperature dependent viscosity and thermal expansion coefficient. *J. Heat Transfer* **100,** 448 (1978).
9. E. R. Lapwood, Convection of a fluid in a porous medium. *Proc. Camb. phil. Soc.* **44,** 508 (1948).
10. F. H. Busse and D. D. Joseph, Heat transfer in a porous layer. *J. Fluid Mech.* **54,** 521 (1972).
11. J. M. Strauss and G. Shubert, Thermal convection of water in a porous medium: effects of temperature and pressure dependent thermodynamic and transport properties. *J. geophys. Res.* **82,** 325–333 (1977).
12. W. J. Minkawycz and P. Chang. Free convection about a vertical flat plate embedded in a porous medium. *Int. J. Heat Mass Transfer* **19,** 805–813 (1977).
13. P. Chang and W. J. Minkawycz, Free convection about a vertical plate embedded in a porous medium with application to heat transfer from a dike. *J. geophys. Res.* **82,** 2040–2044 (1977).
14. C. H. Johnson and P. Chang, Possible similarity solution for free convection boundary layers adjacent to flat plates in porous media. *Int. J. Heat Mass Transfer* **21,** 709–718 (1977).
15. B. Gebhart and J. C. Mollendorf, A new density relation for pure and saline water. *Deep Sea Res.* **24,** 831–841 (1977).
16. J. Ramilison and B. Gebhart, Buoyancy induced transport in porous media saturated with pure or saline water at low temperature. *Int. J. Heat Mass Transfer* **23,** 1521–1530 (1980).
17. B. Gebhart, B. Hassard, S. P. Hastings and N. Kazarinoff, Multiple steady state solutions for buoyancy induced transport in porous media saturated with water. *Numer. Heat Transfer* **6,** 337–352 (1983).
18. S. P. Hastings and N. D. Kazarinoff, Multiple solutions for a problem in buoyancy induced flow. *Archs ration. Mech. Analysis* **89,** 229–249 (1955).
19. C.-A. Wang, Multiple numerical solutions of buoyancy induced flows of a vertical ice wall melting in saturated porous media. *Comput. Math. Applic.* 14(7), 527–540 (1987).
20. L. A. Bromley, V. A. Desaussure, J. C. Clipp and J. S. Wright, Heat capacities of sea water solutions at salinities of 1 to 12% and temperatures of 2 to 80°C. *J. chem. Engng Data* **12,** 202–206 (1967).
21. J. Bear, *Dynamics of Fluid in Porous media*, pp. 647–651. American Elsevier, New York (1972).
22. H. W. Somerton, Some thermal characteristics of porous rocks. *J. Petrol. Technol.* **10**(Note 2008), 61–64 (1958).
23. D. R. Caldwell, Thermal conductivity of sea water. *Deep Sea Res.* **21,** 131–137 (1974).